



The lateral collateral ligament complex of the elbow: quantitative anatomic analysis of the lateral ulnar collateral, radial collateral, and annular ligaments

Christopher L. Camp, MD^{a,*}, Michael Fu, MD^b, Hamidreza Jahandar, MS^c,
Vishal S. Desai, BS^a, Alec M. Sinatro, BA^b, David W. Altchek, MD^b,
Joshua S. Dines, MD^b

^aDepartment of Orthopedic Surgery and Sports Medicine, Mayo Clinic, Rochester, MN, USA

^bSports Medicine and Shoulder Service, Hospital for Special Surgery, New York, NY, USA

^cDepartment of Biomechanics, Hospital for Special Surgery, New York, NY, USA

Background: Injury to the lateral ulnar collateral ligament (LUCL) complex of the elbow often results in posterolateral rotatory instability. Although surgical reconstruction of the LUCL is often required, gaps in our understanding of the LUCL complex remain. The purpose of this study was to provide a robust and accurate characterization of the lateral elbow ligamentous complex.

Methods: The LUCLs, radial collateral ligaments, and annular ligaments in 10 cadaveric elbows were 3-dimensionally digitized and reconstructed using computed tomography. Surface areas, origin and insertion footprint areas, distances between perceived footprint centers and geometric footprint centroids, distances to key landmarks, and ligament isometry were measured.

Results: The mean surface area of the LUCL was 229.3 mm². The mean origin and insertion footprint areas were 26.0 mm² and 22.9 mm², respectively. The mean distance between the apparent centers and the geometric centroids of the footprints was 1 mm. The center of the LUCL origin was 10.7 mm distal to the lateral epicondyle and 8.2 mm from the capitellar articular margin. The center of the LUCL insertion was 3.3 mm distal to the apex of the supinator crest. The LUCL showed anisometric properties as elbow flexion increased ($P < .001$).

Conclusions: The LUCL origin center was 10.7 mm from the lateral epicondyle, whereas the insertion center was 3.3 mm from the apex of the supinator crest. The visually estimated footprint centers were generally within 1 mm of the geometric centroid. These geometries and distances to key landmarks will be informative for surgeons seeking to perform anatomic ligament reconstruction procedures.

Level of evidence: Anatomy Study; Cadaveric Dissection

© 2018 Journal of Shoulder and Elbow Surgery Board of Trustees. All rights reserved.

Keywords: Posterolateral rotatory instability; lateral ligamentous complex of elbow; lateral ulnar collateral ligament; radial collateral ligament; annular ligament; cadaveric

This work was approved by the Hospital for Special Surgery Institutional Review Board (study approval No. 2015-645-CR1).

*Reprint requests: Christopher L. Camp, MD, Mayo Clinic, 200 First St SW, Rochester, MN 55905, USA.

E-mail address: camp.christopher@mayo.edu (C.L. Camp).

In the upper extremity, elbow dislocations are second only to those of the glenohumeral joint, with an estimated incidence of 5.2 dislocations per 100,000 person-years.^{11,23} Most simple elbow dislocations can be successfully treated nonoperatively with closed reduction and bracing; however, recurrent elbow instability, most commonly posterolateral rotatory instability (PLRI), develops in a subset of patients.^{17,19} First described by O'Driscoll et al,¹⁹ PLRI describes a spectrum of instability ranging from subtle posterolateral rotatory subluxation of the radius and ulna away from the humerus to gross, recurrent elbow instability that requires surgical reconstruction.^{4,18}

Biomechanically, PLRI of the elbow occurs secondary to insufficiency of the lateral collateral ligamentous complex, with the lateral ulnar collateral ligament (LUCL) serving as the primary restraint to PLRI.⁵ The remainder of the lateral ligamentous complex is composed of the annular ligament (AL) and radial collateral ligament (RCL),¹⁵ each of which is an important contributor to elbow stability.^{7,13} In addition to traumatic etiologies, the integrity of the lateral ligamentous complex can be compromised in the setting of iatrogenic injury such as lateral elbow surgery, multiple corticosteroid injections, and severe cases of tennis elbow (lateral epicondylitis), or it can manifest in a delayed fashion in patients with cubitus varus deformities.^{1,3,20}

Surgical reconstruction of the LUCL is often indicated in the treatment of recurrent PLRI, and it is generally performed with the goal of restoring native ligament anatomy and isometry.^{2,16} However, certain aspects of the ligament kinematics and bony insertional anatomy have not been completely elucidated. Whereas several historical studies relied on gross inspection, palpation, and caliper measurement of tissue characteristics,^{6,15,21} recent studies have used advanced technology such as electromagnetic sensors and 3-dimensional (3D) computational modeling of magnetic resonance imaging data.^{8,14} These works have reported somewhat conflicting results on the isometry of lateral-sided ligaments.

In addition, the spatial dimensions of the lateral elbow ligament footprints have not been well established, and differences may exist between perceived ligamentous insertions and actual geometric centers of the anatomic footprints.

Therefore, using an established 3D digitizing protocol for making precise spatial measurements, the purpose of this study was to provide a robust and accurate characterization of the lateral elbow ligamentous complex. More specifically, we sought to (1) characterize the lateral elbow ligamentous complex in terms of origin and insertion dimensions, (2) determine discrepancies between the apparent center points of ligament footprints and the true geometric center points, and (3) assess the isometry of the native LUCL through an arc of elbow flexion and extension. We hypothesized that the ligaments' geometries could be reliably quantified, that we could reliably identify footprint centers, and that the LUCL would not be perfectly isometric through flexion and extension.

Materials and methods

Dissection and specimen preparation

Ten unmatched fresh-frozen extremities were dissected down to the level of the joint capsule and LUCL complex. All soft tissue other than the joint capsule, elbow ligaments, and tendinous insertions of the biceps, brachialis, and triceps was discarded (Fig. 1). After removal of extraneous soft tissue, a screw was placed across the distal radioulnar joint while the forearm was placed in full supination. The distal forearm and proximal humerus were potted in Bondo Lightweight Filler 265 (3M, St Paul, MN, USA). In preparation for geometric digitization and co-registration with computed tomography (CT), borosilicate glass spheres (Hartford Technologies, Rocky Hill, CT, USA) were fixed to the humerus and ulna as fiducial markers (Fig. 1). These allowed for co-registration of digitization data with reconstructed 3D bone geometries. Because previous work has shown improved accuracy and reliability of the co-registration process when the spheres are closest to the object they are measuring and are placed out of plane from one another, the spheres were placed close to the

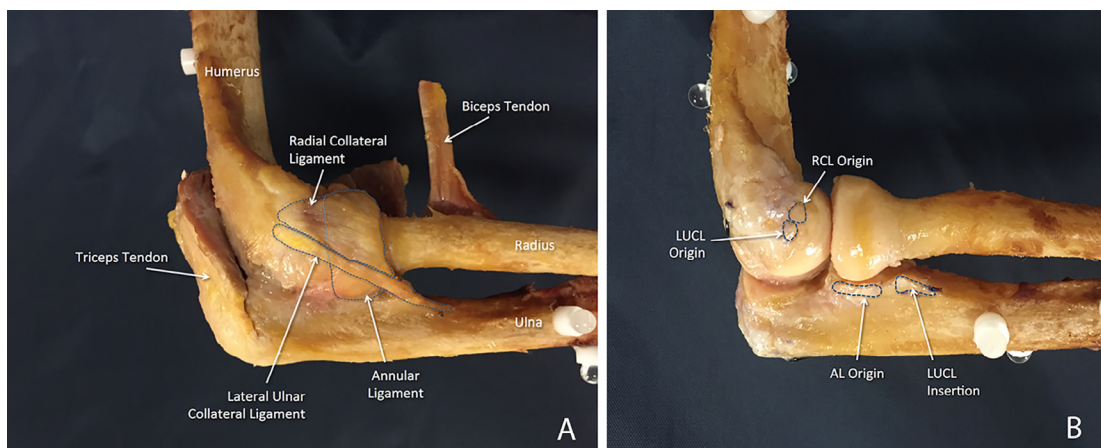


Figure 1 (A) Lateral view of elbow showing intact lateral collateral ligament complex including radial collateral ligament, annular ligament, and lateral ulnar collateral ligament. (B) With the ligamentous complex resected, the origins and insertions of the radial collateral ligament (RCL), lateral ulnar collateral ligament (LUCL), and annular ligament (AL) are outlined.

joint, and no more than 2 spheres were placed in a collinear orientation.²²

Three-dimensional anatomic digitization

All specimens were digitized and co-registered with CT using a previously validated technique.¹² Each specimen was initially set in full extension (as defined by 0° on a goniometer or the full limit of extension for that particular specimen) with the distal forearm securely clamped in place. A 3D coordinate measuring device (FARO Gage; Faro, Orlando, FL, USA) with a known accuracy of 0.018 mm was mounted by a ball probe tip, and the spheres were digitized at 0°, 30°, 60°, and 90° of flexion. Ligamentous structures were outlined with the elbow in 90° of flexion, as shown in [Figure 1](#), and the perimeters and surface areas of each ligament were digitized using a sharp-tipped probe (FARO Gage). The borders of ligaments were carefully identified by using standard osseous anatomic landmarks (lateral epicondyle, radial head, supinator crest, and so on), alterations or changes in fiber orientation (which was particularly important for identifying transition zones between adjacent ligaments), and tissue thickness (which was particularly important for identifying transition zones between the capsule and ligaments, as ligaments showed increased thickness compared with the capsule). Ligaments were subsequently released in their midsubstance to digitize the complete outlines of the origin and insertional footprints of the LUCL and AL. For the RCL, only the origin footprint was digitized, and its insertion onto soft tissue was not digitized. Visual centers of each outlined footprint were digitized by an orthopedic surgeon. This was done to allow assessment of the surgeon's ability and accuracy to visually identify the center of the footprints, which is commonly required when performing surgical reconstruction of these ligaments. The precision and reliability of this technique were assessed using repeated-measurement testing. The process was deemed reliable as all measurements were consistently found to be within 1 mm of one another. Geometric centroids were calculated from the outlines of each digitized footprint by the 3D digitization software. To accomplish this, points were equally distributed around the footprint perimeter in an effort to minimize bias, and the geometric centroids of these points were calculated. The following landmarks were also digitized: lateral epicondyle, apex of supinator crest, tip of coronoid, outline of capitellar articular margin, and outline of coronoid articular margin.

Three-dimensional CT

Before anatomic digitization, all specimens underwent CT with 3D reconstruction. The fiducial markers were maintained throughout the experiment, and this allowed for co-registration of the anatomic measures with the 3D CT images. Digitized ligament anatomy was mapped onto the 3D renderings of both the ulna and humerus for each specimen using the technique of Li et al¹² mentioned earlier. This technique has been documented to register the digitized ligament insertions to within 0.59 mm of the 3D renderings of the underlying bone as generated by CT.¹²

Data analysis

The ligament origin and insertion surface areas were determined from their digitized footprints using techniques described by Harner et al.⁹ All ligament and footprint surface areas were determined with the

elbow placed in 90° of flexion. The footprint length was measured as the maximal distance between the most proximal and distal points of the outline of each footprint.

Statistical analysis

The following outcomes were collected: surface area of LUCL and RCL; origin footprint areas of LUCL, RCL, and AL; insertion footprint areas of LUCL and AL; distance between footprint centers and key bony landmarks; distance between perceived footprint centers and geometric footprint centroids; and ligament isometry through arc of flexion. Descriptive statistics including mean, standard deviation, range, median, and 95% confidence interval were performed on all collected outcome measures. Appropriate hypothesis testing (2-tailed *t* test) was performed to assess the significance of differences in the mean distance between the origin and insertion centers of the LUCL during full extension (0°) and 90° of elbow flexion. $P \leq .05$ denoted statistical significance.

Results

The overall surface area of the LUCL was 229.3 ± 35.9 mm², with mean origin and insertion footprint areas of 26.0 ± 5.9 mm² and 22.9 ± 7.8 mm², respectively. The mean surface area of the RCL was the largest of all ligaments, measuring 292.1 ± 79.5 mm². The AL had the largest insertional footprint of the lateral ligamentous complex, measuring 36.6 ± 13.0 mm². Additional dimension measurements are shown in [Table I](#) and illustrated in [Figure 2](#).

The insertional footprint of the LUCL was shown to be independent of and distal to the AL footprint. It consistently showed a tapered shape with a distal elongation ([Fig. 2](#)). The mean distances between the apparent center of the LUCL origin or insertional footprints and their geometric centroids were 1.1 ± 0.4 mm and 1.1 ± 0.3 mm, respectively. Data for all 3 ligaments are presented in [Table II](#).

[Figure 3](#) shows the mean distances between the centers of the measured footprints and notable bony landmarks on the humerus and ulna. The mean distance from the apex of the lateral epicondyle to the center of the origins of the LUCL and RCL was 10.7 ± 3.3 mm and 7.3 ± 1.2 mm, respectively. The center of the insertion of the LUCL was a mean distance of 3.3 ± 2.3 mm distal to the apex of the supinator crest, which typically marked the proximal-most aspect of the LUCL insertion. The center of the insertional footprint of the AL was a mean distance of 14.2 ± 1.9 mm from the tip of the coronoid ([Fig. 3](#)). The LUCL did not show isometric properties as the mean distance between the centers of the ligament origin and insertional footprints increased 2.6 mm when the lengths at 0° and 90° of elbow flexion were compared ($P < .001$) ([Table III](#)).

Discussion

In this investigation, the LUCL insertional footprint center was 3.3 mm distal to the apex of the supinator crest, was

Table I Surface areas of ligaments, origins, and insertions of lateral collateral ligament complex for each ligament

Structure	Area, mm ²			
	Mean	SD	Range	Median
Lateral ulnar collateral ligament				
Ligament surface	229.3	35.9	180.5-288.2	223.8
Origin	26.0	5.9	15.9-33.7	27.4
Insertion	22.9	7.8	13.2-40.0	21.7
Radial collateral ligament				
Ligament surface	292.1	79.5	208.4-443.8	285.1
Origin	31.6	10.0	15.7-53.8	29.8
Annular ligament				
Origin	25.7	17.4	12.6-60.5	19.3
Insertion	36.6	13.0	21.7-56.3	31.3

SD, standard deviation.

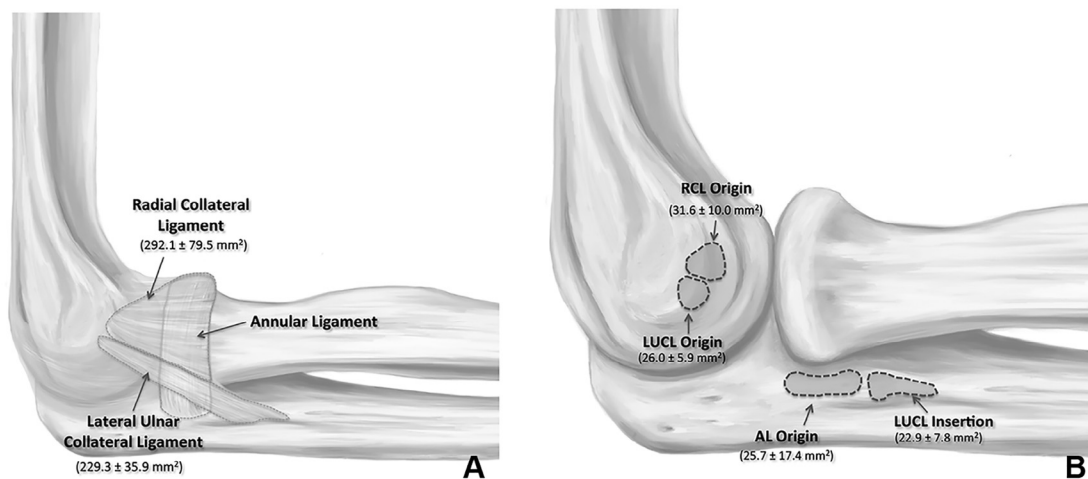


Figure 2 (A) Total area of intact ligaments of lateral elbow including radial collateral ligament and lateral ulnar collateral ligament. (B) Areas of origin and insertional footprints of radial collateral ligament (RCL), annular ligament (AL), and lateral ulnar collateral ligament (LUCL).

Table II Comparison of distances between apparent centers of ligament footprints and geometric centroids

	Distance, mm			
	Mean	SD	Range	Median
Lateral ulnar collateral ligament				
Origin	1.1	0.4	0.4-1.5	1.2
Insertion	1.1	0.3	0.5-1.4	1.2
Radial collateral ligament				
Origin	1.1	0.3	0.5-1.6	1.1
Annular ligament				
Origin	1.0	0.3	0.7-1.7	0.9
Insertion	2.2	1.5	0.6-6.3	1.8

SD, standard deviation.

consistently tapered in shape, and was independent of the AL origin. The LUCL did not show true isometry as it lengthened 2.6 mm from 0° to 90° of elbow flexion. For both LUCL footprints, the distance between the digitized apparent center

and the calculated geometric center was low, at 1.1 mm. Because the goal of LUCL reconstruction is to achieve elbow stability through restoration of native ligament anatomy and kinematics, these spatial characteristics of the ligamentous footprints and surface areas may prove beneficial to surgeons.

In the lateral elbow, the LUCL fibers extend distally to blend with the AL; however, they then separate to form a distinct insertion onto the proximal ulna at the supinator crest (Figs. 1 and 2). The kinematic properties of the reconstructed ligament may be significantly altered if a large difference exists between the apparent center of the LUCL footprint and the measured geometric centroid of the insertion. However, in this study, a mean difference between these 2 points of just 1.1 mm (range, 0.5-1.4 mm) was observed, suggesting that surgeons should be able to reliably approximate the geometric center of the ligament insertion. When the ligament is chronically attenuated or disrupted and the boundaries of the footprint are not clear, it may be best for the surgeon to rely on the distances between the footprints and key bony landmarks. In addition, a number of factors can be used to assist

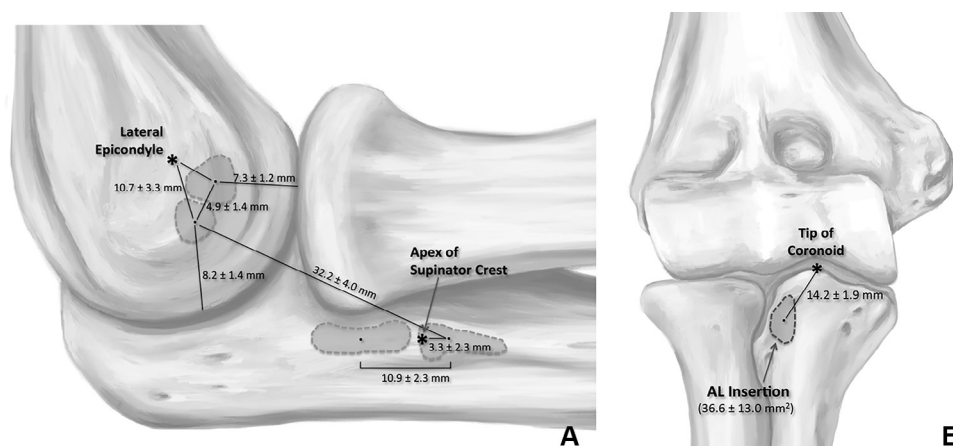


Figure 3 Distance between footprint centers and key landmarks on lateral (A) and anterior (B) aspects of elbow. AL, annular ligament.

Table III Distance between centers of ligament origin and insertional footprints at varying degrees of elbow flexion

Lateral ulnar collateral ligament	Distance, mm						<i>P</i>
	Mean	SD	Range	Median	MD*	95% CI	
0° of flexion	29.6	3.7	22.3-35.4	29.8	2.6	-1.02 to 6.22	<.001
30° of flexion	29.9	3.7	22.6-35.3	31.0			
60° of flexion	30.4	4.3	20.9-36.2	32.0			
90° of flexion	32.2	4.0	23.1-38.0	32.9			

SD, standard deviation; MD, mean difference; CI, confidence interval.

* Calculated between 0° and 90° of elbow flexion.

surgeons in precisely identifying the LUCL insertion, including its distinct insertion just distal to the AL origin, proximal border originating along the apex of the supinator crest, and center point located 3.3 mm distal to this apex.

In addition, this work showed that through an elbow flexion arc of 0° to 90°, the LUCL was not a truly isometric structure, ranging from 29.6 mm in length at 0° to 32.2 mm at 90°. There is some disagreement in the literature regarding the isometry of the LUCL. In terms of identifying the isometric point of the LUCL and performing LUCL reconstruction, some authors have reported that the most isometric origin of the LUCL is at the geometric center of the curvature of the capitellum²⁴ whereas others have found the isometric point to be 2 mm proximal to the center of the capitellum.¹⁴ In our study, the center of the LUCL origin footprint was equidistant from the articular margin of the capitellum, but the ligament itself was not isometric. In a cadaveric elbow study examining possible humeral and ulnar fixation sites for LUCL reconstruction, Goren et al⁸ were unable to locate truly isometric LUCL tunnel positions. In our investigation, the center of the footprint was located 10.7 mm distal to the lateral epicondyle, 8.2 mm proximal to the articular margin of the capitellum, and 4.9 mm posterior to the center of the RCL origin. These additional data points should be taken into consideration when attempting to locate the center of the footprint during surgical repair or reconstruction. Although the results of this study using 3D digitizing technology suggest that

anisometry exists between the centers of the footprints of the native LUCL, most surgeons attempt to achieve relative isometry when performing LUCL reconstruction.^{1,2,5,10,16} Further studies are needed to compare the kinematics and clinical outcomes of truly anatomic versus isometric LUCL reconstructions.

This work is subject to several important limitations that merit discussion. First, there is potential bias in the positions of the apparent footprint centers and, to a lesser extent, the geometric centroid of the ligament footprints. Although repeated-measures testing showed accuracy and reliability within 1 mm, this small margin of error could have an impact on the results. In addition, the anatomic dimensions of the structures examined in this study may vary significantly based on patient sex, hand dominance, activity level, and size, as evidenced by the large ranges for some of the variables. An a priori power analysis was not performed to determine the number of specimens necessary to achieve statistical significance. Similarly, our sample size was not adequately powered to perform subanalyses based on the aforementioned specimen variables, and further studies examining these anatomic differences may help guide personalized reconstructions based on patient characteristics. Finally, although the distance between the apparent LUCL insertion footprint center and the geometric centroid was only 1.1 mm, it is unclear whether this difference in ulnar fixation position would have a significant effect on the biomechanical properties of LUCL reconstruction.

Conclusion

The LUCL origin center was 10.7 mm from the lateral epicondyle, whereas the insertion center was 3.3 mm from the apex of the supinator crest. The visually estimated footprint centers were generally within 1 mm of the geometric centroid. These geometries and distances to key landmarks will be informative for surgeons seeking to perform anatomic ligament reconstruction procedures.

Disclaimer

This work was funded by internal institutional funds including the Hospital for Special Surgery Shoulder and Sports Medicine Research Fund and the Surgeon in Chief Fund, the Clark Foundation, the Kirby Foundation, and the Gosnell Family.

The authors, their immediate families, and any research foundations with which they are affiliated have not received any financial payments or other benefits from any commercial entity related to the subject of this article.

References

1. Anakwenze OA, Kancherla VK, Iyengar J, Ahmad CS, Levine WN. Posterolateral rotatory instability of the elbow. *Am J Sports Med* 2014;42:485-91. <http://dx.doi.org/10.1177/0363546513494579>
2. Anakwenze OA, Kwon D, O'Donnell E, Levine WN, Ahmad CS. Surgical treatment of posterolateral rotatory instability of the elbow. *Arthroscopy* 2014;30:866-71. <http://dx.doi.org/10.1016/j.arthro.2014.02.029>
3. Camp CL, O'Driscoll SW, Wempe MK, Smith J. The sonographic posterolateral rotatory stress test for elbow instability: a cadaveric validation study. *PM R* 2017;9:275-82. <http://dx.doi.org/10.1016/j.pmrj.2016.06.014>
4. Camp CL, Sanchez-Sotelo J, Shields MN, O'Driscoll SW. Lateral ulnar collateral ligament reconstruction for posterolateral rotatory instability of the elbow. *Arthrosc Tech* 2017;6:e1101-5. <https://doi.org/10.1016/j.eats.2017.03.029>
5. Charalambous CP, Stanley JK. Posterolateral rotatory instability of the elbow. *J Bone Joint Surg Br* 2008;90:272-9. <http://dx.doi.org/10.1302/0301-620X.90B3.19868>
6. Cohen MS, Hastings H II. Rotatory instability of the elbow. The anatomy and role of the lateral stabilizers. *J Bone Joint Surg Am* 1997;79:225-33.
7. Dunning CE, Zarzour ZD, Patterson SD, Johnson JA, King GJ. Ligamentous stabilizers against posterolateral rotatory instability of the elbow. *J Bone Joint Surg Am* 2001;83:1823-8.
8. Goren D, Budoff JE, Hipp JA. Isometric placement of lateral ulnar collateral ligament reconstructions: a biomechanical study. *Am J Sports Med* 2010;38:153-9. <http://dx.doi.org/10.1177/0363546509346049>
9. Harner CD, Baek GH, Vogrin TM, Carlin GJ, Kashiwaguchi S, Woo SL. Quantitative analysis of human cruciate ligament insertions. *Arthroscopy* 1999;15:741-9.
10. Jones KJ, Dodson CC, Osbahr DC, Parisien RL, Weiland AJ, Altchek DW, et al. The docking technique for lateral ulnar collateral ligament reconstruction: surgical technique and clinical outcomes. *J Shoulder Elbow Surg* 2012;21:389-95. <http://dx.doi.org/10.1016/j.jse.2011.04.033>
11. Kuhn MA, Ross G. Acute elbow dislocations. *Orthop Clin North Am* 2008;39:155-61, v. <http://dx.doi.org/10.1016/j.ocl.2007.12.004>
12. Li K, O'Farrell M, Martin D, Kopf S, Harner C, Zhang X. Mapping ligament insertion sites onto bone surfaces in knee by co-registration of CT and digitization data. *J Biomech* 2009;42:2624-6. <http://dx.doi.org/10.1016/j.jbiomech.2009.06.042>
13. McAdams TR, Masters GW, Srivastava S. The effect of arthroscopic sectioning of the lateral ligament complex of the elbow on posterolateral rotatory stability. *J Shoulder Elbow Surg* 2005;14:298-301. <http://dx.doi.org/10.1016/j.jse.2004.08.003>
14. Moritomo H, Murase T, Arimitsu S, Oka K, Yoshikawa H, Sugamoto K. The in vivo isometric point of the lateral ligament of the elbow. *J Bone Joint Surg Am* 2007;89:2011-7. <http://dx.doi.org/10.2106/JBJS.F.00868>
15. Morrey BF, An KN. Functional anatomy of the ligaments of the elbow. *Clin Orthop Relat Res* 1985:84-90.
16. Nestor BJ, O'Driscoll SW, Morrey BF. Ligamentous reconstruction for posterolateral rotatory instability of the elbow. *J Bone Joint Surg Am* 1992;74:1235-41.
17. O'Brien MJ, Savoie FH 3rd. Arthroscopic and open management of posterolateral rotatory instability of the elbow. *Sports Med Arthrosc* 2014;22:194-200. <http://dx.doi.org/10.1097/JSA.000000000000029>
18. O'Driscoll SW. Classification and evaluation of recurrent instability of the elbow. *Clin Orthop Relat Res* 2000;370:34-43.
19. O'Driscoll SW, Bell DF, Morrey BF. Posterolateral rotatory instability of the elbow. *J Bone Joint Surg Am* 1991;73:440-6.
20. O'Driscoll SW, Spinner RJ, McKee MD, Kibler WB, Hastings H II, Morrey BF, et al. Tardy posterolateral rotatory instability of the elbow due to cubitus varus. *J Bone Joint Surg Am* 2001;83:1358-69.
21. Regan WD, Korinek SL, Morrey BF, An KN. Biomechanical study of ligaments around the elbow joint. *Clin Orthop Relat Res* 1991:170-9.
22. Soderkvist I, Wedin PA. Determining the movements of the skeleton using well-configured markers. *J Biomech* 1993;26:1473-7.
23. Stoneback JW, Owens BD, Sykes J, Athwal GS, Pointer L, Wolf JM. Incidence of elbow dislocations in the United States population. *J Bone Joint Surg Am* 2012;94:240-5. <http://dx.doi.org/10.2106/JBJS.J.01663>
24. Streubel PN, Cohen MS. Posterolateral rotatory instability of the elbow: diagnosis and surgical treatment. *Oper Tech Sports Med* 2014;22:190-7. <https://doi.org/10.1053/j.otsm.2014.02.014>